2020 IEEE 17th International Symposium on Biomedical Imaging (ISBI)
April 3-7, 2020, Iowa City, Iowa, USA

A TEMPORAL MODEL FOR TASK-BASED FUNCTIONAL MR IMAGES

Claire Yilin Lin[⋆] *Douglas C. Noll*[†] *Jeffrey A. Fessler*[‡]

[⋆]Mathematics, [†]BME, and [‡]EECS Departments, University of Michigan, MI, USA

ABSTRACT

To better identify task-activated brain regions in task-based functional magnetic resonance imaging (tb-fMRI), various space-time models have been used to reconstruct image sequences from k-space data. These models decompose a fMRI timecourse into a static background and a dynamic foreground, aiming to separate task-correlated components from non-task signals. This paper proposes a model based on assumptions of the activation waveform shape and smoothness of the timecourse, and compare it to two contemporary tb-fMRI decomposition models. We experiment in the image domain using a simulated task with known region of interest, and a real visual task. The proposed model yields fewer false activations in task activation maps.

1. INTRODUCTION

Improving spatial and temporal resolution in fMRI will likely require better dynamic image reconstruction from undersampled k-space data. In particular, acceleration of fMRI data acquisition achieved by parallel imaging has led to reconstruction models based on sparsity and low-rank assumptions [1]-[4]. In addition to confounding factors such as physiological noise, scanner drift, and motion effects, challenges in fMRI reconstruction also arise in the choice of model assumptions and cost function formulation. With different aims in the timecourse analysis of task-based and resting state fMRI, it is desirable to develop models that address specific needs.

This paper considers task-based fMRI (tb-fMRI), with the goal to detect task-activated regions of the brain. Traditional image analysis involves preprocessing the reconstructed images to correct for noise and artifacts, then comparison with a predefined hemodynamic response function (HRF)-convolved activation waveform using general linear modeling (GLM) [5]. To obtain a model appropriate for tb-fMRI, we consider different cost functions in the image space, taking into account *a priori* knowledge of the task and blood oxygenation level dependent (BOLD) signal behaviors. We then propose a model based on temporal smoothness assumption, and show that it better recovers the image sequence and timecourse on fMRI datasets with simulated and real tasks than several other temporal models.

Supported in part by NIH grant R01 EB023618.

2. FMRI MODELS

Our long-term goal is to develop spatio-temporal models for whole-brain fMRI signals that are suitable for image reconstruction from undersampled k-space data. To investigate various models, we start with "fully sampled" fMRI data over a small brain slab that has been reconstructed frame by frame to yield an image series. We then retrospectively undersample those dynamic images, and investigate how well various space-time models can perform the matrix completion problem of recovering the original series of images from the undersampled image data:

$$\underset{X}{\operatorname{argmin}} \frac{1}{2}\|\mathbf{\Omega}X - d\|_2^2 + \lambda R(X), \tag{1}$$

where $X \in \mathbb{C}^{N_x N_y \times N_t}$ is the desired image sequence, $\mathbf{\Omega} : \mathbb{C}^{N_x N_y \times N_t} \to \mathbb{C}^{N_s}$ is a spatial and temporal random undersampling operator, $d \in \mathbb{C}^{N_s}$ is the undersampled image, and $R(\cdot)$ is a regularizer with parameter λ that depends on the space-time model assumptions.

The motivation for (1) is to investigate models that can recover the image even in the presence of spatial and temporal undersampling, while relieving the computational burden and algorithm complexity of solving a reconstruction problem from k-space. Here we obtain d by reconstructing images from fully sampled k-space data and then retrospectively undersample with $\mathbf{\Omega}$. We then compare (1) with different underlying assumptions, and present their corresponding cost functions, optimization schemes, and fMRI task performance.

2.1. Existing Models

This section reviews two existing reconstruction models for tb-fMRI in the framework of (1), with underlying assumptions leading to the proposed model in the next section.

2.1.1. Low-Rank Plus Sparse (L+S) Decomposition

The low-rank plus sparse (L+S) approach [2],[3] models fMRI image as $X = L + S$, where the low-rank component L models the non-task temporally correlated background, and the sparse component S models the pseudo-periodic BOLD activity. With these assumptions in the image domain,

problem (1) becomes

$$\underset{L,S}{\operatorname{argmin}} \frac{1}{2}\|\mathbf{\Omega}(L+S)-d\|_2^2+\lambda_L\|L\|_*+\lambda_S\|\mathbf{T}S\|_1, \quad (2)$$

where $\mathbf{T}:\mathbb{C}^{N_xN_y\times N_t}\rightarrow\mathbb{C}^{N_xN_yN_t}$ is the (unitary) temporal Fourier transform operator. The nuclear norm encourages L to be low-rank, and the l_1 norm encourages S to be periodic. We solve (2) by alternating between two proximal gradient updates, with singular value thresholding (SVT) for L and soft thresholding for S.

2.1.2. Low-Rank Plus Task-Based Decomposition (L+UV)

Instead of using temporal-Fourier-transformed sparsity as a regularizer, [4] considers a spatial-temporal decomposition UV, where $U\in\mathbb{C}^{N_xN_y\times N_r}$ is an estimated spatial map corresponding to a predefined temporal basis $V\in\mathbb{C}^{N_r\times N_t}$, where N_r is the number of task-associated basis vectors. Here V can be a HRF-convolved waveform, or more generally a sinusoidal or block-like function, along with its temporal derivative. Compared with the L+S model, the temporal basis V further constrains the shape of activation signal. In the image space the minimization problem (1) now becomes

$$\underset{L,U}{\operatorname{argmin}} \frac{1}{2}\|\mathbf{\Omega}(L+UV)-d\|_2^2+\lambda_L\|L\|_*, \quad (3)$$

which has one fewer regularization parameter to tune than (2). We again solve (3) by alternating minimization, updating L by SVT and U by closed-form linear least squares update.

2.2. Proposed Model: Smooth Background Plus Spatial-Temporal Decomposition (B+UV)

Both (2) and (3) assume that a timecourse can be decomposed into a temporally static background and a dynamic foreground, with incoherence between the two. However, incoherence of L and S in (2) might not apply to tb-fMRI, where the block-like task activation has low rank. The temporal basis in (3), on the other hand, aims to separate the two components with *a priori* information of the activation waveform, to specify an expected shape of the activation.

Building on the idea of decomposition with a predefined temporal basis, we propose to model the image as $X=B+UV$, with B smoothly varying across time, and UV capturing activation and general trend of the timecourse. In addition to the activation waveform in V, we consider a column of all ones to account for the mean, and a linearly spaced vector for scanner drift, a typical artifact in MRI scans.What we expect to be left in B is then the background BOLD signal, likely confounded by physiological and motion noise. For the tb-fMRI goal of identifying task-activated brain regions, we consider a smoothness assumption on the background signal B by applying a regularizer $\|\mathbf{D}B\|_2^2$, where $\mathbf{D}:\mathbb{C}^{N_xN_y\times N_t}\rightarrow\mathbb{C}^{N_xN_yN_t}$ is a temporal finite difference operator. Our new cost function is then

$$\underset{B,U}{\operatorname{argmin}} \frac{1}{2}\|\mathbf{\Omega}(B+UV)-d\|_2^2+\lambda_B\|\mathbf{D}B\|_2^2. \quad (4)$$

Since different voxels can have different slopes in the linear drift component, including it in UV is advantageous over in B, where the difference between timepoints is regularized by the same parameter λ_B for all voxels.

We solve (4) by alternating update of B and U, with conjugate gradient or gradient descent for B, and closed-form least squares update for U.

3. RESULTS

To compare the models on tb-fMRI images, we use two fMRI datasets of healthy volunteers, collected on a GE 3T MRI scanner with a 32-channel receiver. All human subject experiments were conducted with IRB approval and with informed consent. Our first experiment uses a non-task fMRI dataset, with a simulated activation waveform imposed on a specified region of interest (ROI). The second experiment is real tb-fMRI with a visual checkerboard task. For each dataset, we apply inverse Fourier transform to fully sampled k-space data, and perform complex coil combinations using coil sensitivity maps computed with ESPIRiT [6] to obtain image sequence $D\in\mathbb{C}^{N_xN_y\times N_t}$. We then randomly undersample D in space and time to get $d=\mathbf{\Omega}D$.

We solve for image X with models (2), (3), and (4) by sweeping across and selecting regularization parameters that give the lowest total false positive plus false negative thresholded activation. We then sweep across a range of thresholds and compute the true positive ratio among activated voxels and false positive ratio among non-activated voxels. We show the timecourse results of a task-related and a non-task voxel. We then use linearly detrended D and $L+S$ and u_1, the first column of U in the UV factorization by the L+UV and B+UV models, to compute ROC (receiver operating characteristic) curves of true positive vs. false positive ratios. Finally, we pick a false positive ratio and plot the corresponding maps.

3.1. Simulated Task

For this non-task dataset we use a spiral trajectory with TR = 720 ms, and obtain an image sequence $D\in\mathbb{C}^{100\cdot100\times300}$ with practical noise such as scanner drift and physiological motion. We then add a scaled activation waveform shown in Fig. 1 to a center ROI as a ground truth activated region, and randomly undersample 30% of D to get d.

Fig. 2 shows timecourses of two voxels after parameter sweeping and applying the three models in Section 2. The L+S model has two regularization parameters to tune, and is very sensitive to their values. In addition, S might not capture the activation with the temporal Fourier sparsity assumption,

especially when the activation is weak compared to background BOLD signal and noise, as shown in this case. Compared with L+S, here the L+UV model better separates background and activation, with L capturing non-task-correlated signals. For the proposed B+UV model, UV contains linear and task components, and the timecourse $|B+UV|$ resembles $|D|$ with temporal smoothing, due to our model assumptions.

Fig. 3 shows the ROC curves and activation maps thresholded at 10^{-3} false positive ratio. Both the L+UV and B+UV models give ROC curves and u_1 maps similar to the correlation map of D, while the L+S model produces many more false negative activations. This aligns with observations from timecourses, where Fourier sparsity assumption on S in L+S causes non-task periodic behaviors. The B+UV model, on the other hand, controls the activation shape by the task basis, while avoiding overfitting by smoothness assumption on B.

3.2. Visual Task

We acquire a tb-fMRI dataset using a spiral-in trajectory with TR = 50 ms. The task is an interleave of 20 seconds of left and 20 seconds of right visual checkerboards task, repeated five times. The waveform in Fig. 4 convolves the HRF with a rectangular function that has value -1 for the left visual task, and 1 for the right. After getting an image sequence using sensitivity map, we undersample $D \in \mathbb{C}^{64\cdot64\times4000}$ by 50% to evaluate the models.

Fig. 5 shows timecourses of an activated and a non-activated voxel. The activated voxel corresponds to a right visual task, with anti-correlation to our left visual activation waveform. The L+S model captures some task-activated signal in the S component, although without predefined task information, the periodic behavior looks less similar to the activation waveform. Here the L+UV model does not separate the task-related signal from background signal; because of low-rankness of both components, L and UV can become anti-correlated. Result from the B+UV model agrees with its assumption, with linear trend and activation in UV, which slightly exhibits a quadratic shape here due to the magnitude operation. After adding the B component, the overall timecourse has a temporally smooth behavior. In this case with the large number of timepoints $N_t = 4000$, the B+UV model is also more computationally efficient, as it does not involve an expensive singular value decomposition (SVD) for the low-rank component in the other two models.

To define "ground truth" in this case, we use linearly detrended D as a reference to compute ROC curves and activation maps (thresholded at 10^{-3} false positive ratio) in Fig. 6 for the visual tasks. The L+S assumption results in some false negatives, as in the simulated task case. Similarly, more false positive activations occur with L+UV due to its temporal basis assumption. Among the three, B+UV most resembles a temporally smoothed, but not oversmoothed, version of D.

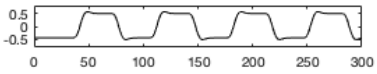

Fig. 1. Simulated activation waveform across 300 timepoints.

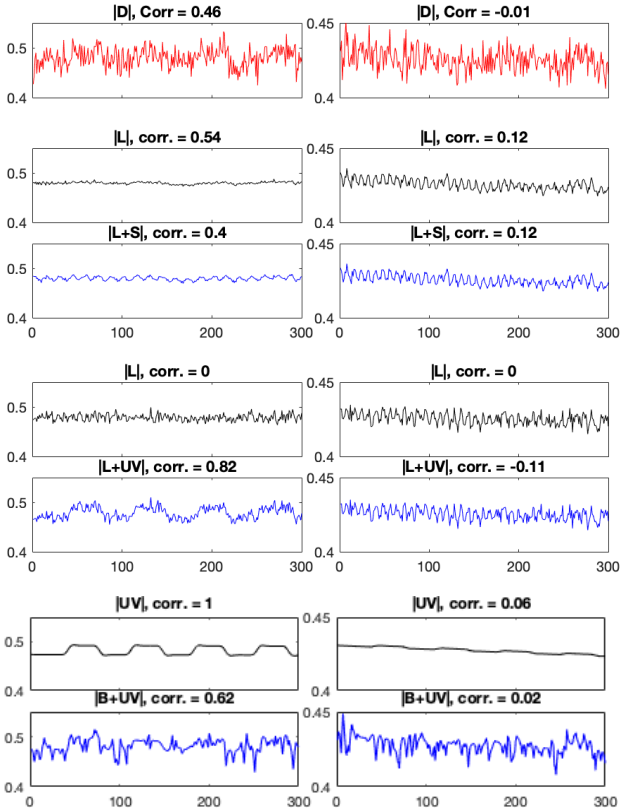

Fig. 2. Timecourses of a task-imposed voxel (left column) and a random voxel (right column) of image sequence D and selected image components using three models, with their correlations to the simulated activation waveform.

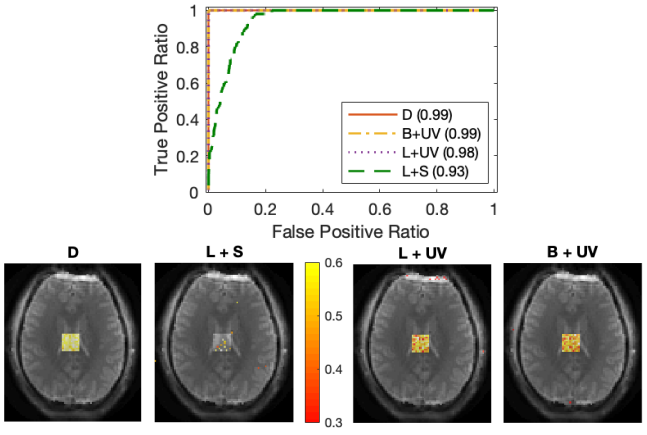

Fig. 3. Top: ROC curves with Area Under Curve (AUC) values for simulated task; Bottom: correlation maps of detrended D and $L + S$, and u_1 maps of L+UV and B+UV models.

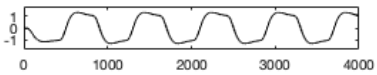

Fig. 4. Visual activation waveform across 4000 timepoints.

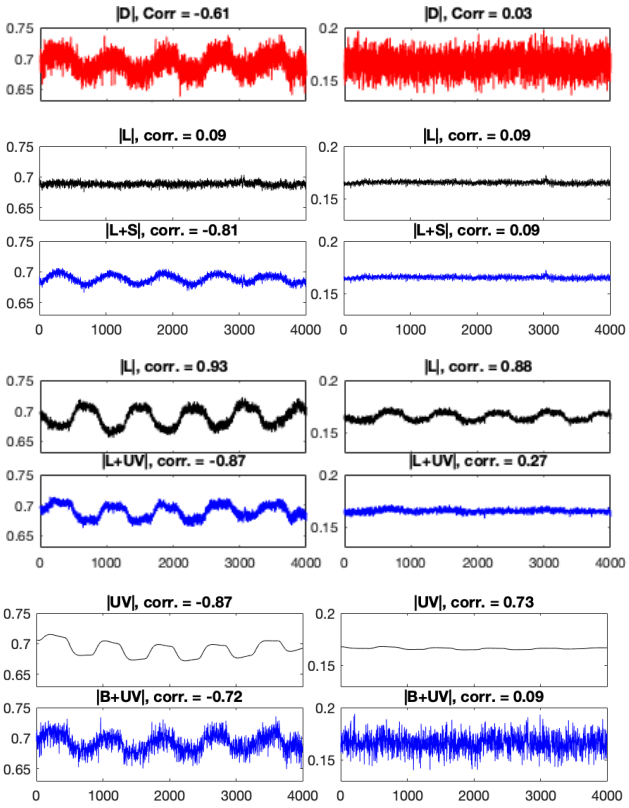

Fig. 5. Timecourses of a right-visual-activated voxel (left column) and a non-task voxel (right column) of image sequence D and selected image components using three models, with their correlations to the visual activation waveform.

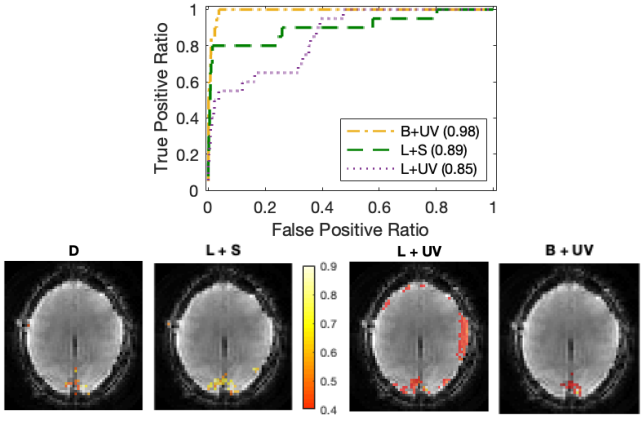

Fig. 6. Top: ROC curves with AUC values for visual task; Bottom: correlation maps of detrended D and $L + S$, and u_1 maps of L+UV and B+UV models.

4. DISCUSSION AND FUTURE WORK

This paper presents a model for tb-fMRI, with an aim to detect task-activated brain regions. Our proposed B+UV model considers temporal linear trend and a predefined activation waveform shape, with temporal smoothness assumption on the background BOLD signal. This model can be extended to more complicated tasks, for example, by including multiple waveforms in the temporal basis matrix V.

Compared with existing tb-fMRI models, the proposed method gives more accurate activation detection with fewer false positives and false negatives. From the minimization problem's standpoint, it is less sensitive to regularization parameter choice than the L+S model. The L+UV model, as implemented in [4], requires specifying a rank for L, and the threshold varies across iterations, resulting in a "moving target" cost function with different λ_L values. Our B+UV model, on the other hand, has a cost function with one regularization parameter, and can be alternatingly minimized with closed form updates.

Future work will extend this model to reconstruction from k-space, with validation using more practical undersampling patterns. With a more complicated system operator that considers coil sensitivity and sampling trajectory, we will also develop fast algorithms for the optimization problem.

5. ACKNOWLEDGEMENT

We thank Amos Cao and Shouchang Guo at the University of Michigan for the fMRI datasets.

6. REFERENCES

[1] H. Jung and J. C. Ye, "Performance evaluation of accelerated functional MRI acquisition using compressed sensing," *IEEE ISBI*, pp. 702–705, 2009.

[2] R. Otazo, A. Franco, J. Chen, C. Marmar, and F. Boada, "Low-rank plus sparse (L+S) decomposition for separation of subsampled physiological noise in fMRI," *OHBM*, vol. 1690, p. 2015, 2015.

[3] V. Singh, A. H. Tewfik, and D. B. Ress, "Under-sampled functional MRI using low-rank plus sparse matrix decomposition," *IEEE ICASSP*, pp. 897–901, 2015.

[4] M. Chiew, N. N. Graedel, and K. L. Miller, "Recovering task fMRI signals from highly under-sampled data with low-rank and temporal subspace constraints," *NeuroImage*, vol. 174, pp. 97–110, 2018.

[5] M. M. Monti, "Statistical analysis of fMRI time-series: a critical review of the GLM approach," *Front. Hum. Neurosci.*, vol. 5, p. 28, 2011.

[6] M. Uecker, P. Lai, M. J. Murphy, P. Virtue, M. Elad, J. M. Pauly, S. S. Vasanawala, and M. Lustig, "ESPIRiT an eigenvalue approach to autocalibrating parallel MRI: where SENSE meets GRAPPA," *Mag. Res. Med.*, vol. 71, pp. 990–1001, 2014.